Two-zone Hall thruster breathing mode mechanism, Part I: Theory

IEPC-2019-354

Presented at the 36th International Electric Propulsion Conference
University of Vienna, Austria
September 15–20, 2019

Ethan T. Dale* and Benjamin A. Jorns†
University of Michigan, Ann Arbor, MI 48109

A theory describing a two-zone breathing mode mechanism is presented. The stability of Hall thrusters is poorly understood in large part to the breathing mode, ubiquitous low-frequency discharge current oscillations. Many theories have already been presented to characterize this instability, yet even the most prominent ones fall short of providing an intuitive analytical description. The prominent predator-prey model of the breathing mode is examined and a two-zone modification of it, involving coupled ionization instabilities near the anode and in the traditional ionization region, is proposed. This model is explored analytically with a linear perturbation analysis. The stability of the system is examined in various limits. A numerical study is performed using approximate steady-state plasma and neutral parameters, and large regions of positive growth are found as the electron near-anode speed and neutral gas channel transit time are varied. In particular, for electron speeds near 2 km/s, real frequencies up to 7 kHz and growth rates near 17 MHz are found. Both quantities are found to be sensitive to the neutral density phase lag, in agreement with additional simplified studies of the predator-prey model. Finally, several criteria for validating this model experimentally are provided.

*Ph.D Candidate, Department of Aerospace Engineering, etdale@umich.edu
†Assistant Professor, Department of Aerospace Engineering

Nomenclature

f_{iz} = ionization frequency, Hz
I_d = discharge current, A
L = characteristic ionization length, m
n = plasma density, m^{-3}
n_a = plasma near-anode density, m^{-3}
n_n = neutral density, m^{-3}
$n_{n,a}$ = neutral near-anode density, m^{-3}
$n_{n,0}$ = injected neutral density, m^{-3}
u_e = electron velocity, m/s
t = time, s
$u_{e,a}$ = electron near-anode velocity, m/s
u_i = ion velocity, m/s
u_n = neutral density, m/s
z = axial position, m
γ = angular growth rate, rad/s
θ_n = plasma density phase lag, rad
θ_{n_n} = neutral density phase lag, rad
λ_D = Debye length, m
ξ_{iz} = ionization rate coefficient, m^3/s
ω = angular frequency, rad/s

I. Introduction

Hall thrusters are a form of electric propulsion that use crossed electric and magnetic fields to produce a plasma and accelerate it for the purpose of generating thrust. These devices are already widely deployed in near-Earth applications where their high specific impulse and moderate thrust density is well-suited to stationkeeping. They are increasingly being projected for deep-space missions.[1]

Since Hall thrusters are designed to operate for long durations – state-of-the-art lifetimes exceed 10,000 hours – the reliability of this technology is critical to its successful implementation. At a minimum, the stability of a thruster must be well-understood to guarantee nominal operation during in-space service. However, there are many aspects of the physical processes governing the operation of Hall thrusters that are still poorly understood. One of the most significant of these that directly impacts stability of these devices are low-frequency discharge current oscillations, termed the "breathing mode".

Despite several decades of theoretical, numerical, and analytical study, the underlying mechanism controlling the growth and onset of the breathing mode is still opaque. Many hypotheses have been proposed but often they are limited by complexity, physical inconsistencies, or vagueness. As a result, the low-frequency stability of Hall thrusters cannot be predicted or intuitively understood. The need is apparent for an evaluation of these existing theories for the purpose of synthesizing a new one that overcomes their deficits. A more accurate description of the breathing mode would improve the understanding of Hall thruster stability, thereby making this form of propulsion more reliable and suitable for new mission spaces.

In this work, Section II will review existing theories for the breathing mode and highlight their successes and failures. In Section III, a new mechanism for the breathing mode is proposed and treated analytically. This theory is evaluated numerically in Section IV. The implications of these results are covered in Section V, as well as potential strategies for experimental validation of the proposed mechanism. The validation will be addressed further in Part II of this study, Ref. 2. Finally, the entire work is summarized in Section VI.

II. Background

The breathing mode has been studied experimentally[3–7] and resolved numerically,[8–11] yet there is no intuitive but rigorous analytical description for its onset and growth. An early theory for low-frequency oscillations proposed by Fife et al. is the predator-prey model.[12] This description has remained a prominent qualitative explanation for oscillatory behavior to the present day. Work by Barral and Ahedo has proposed a more comprehensive ionization instability for the breathing mode.[13] Finally, numerical studies have recently suggested that other regions in the plasma aside from the typical ionization zone may play an important role in the breathing process. All of these models and findings will now be reviewed.

A. Predator-Prey

The predator-prey model was proposed to accompany 1D hybrid particle-in-cell simulations of a Hall thruster by Fife et al.[12] A cyclic depletion of neutral particles was likened to a Lotka-Volterra, or predator-prey, process where neutrals are prey and electrons are predators. Physically, as the thruster channels fills with neutral particles, the ionization rate increases and thus the plasma thickens. As the electron density rises, avalanche ionization occurs such that the neutral population is rapidly reduced. Ionization then decreases while plasma continues to be accelerated out of the channel, yielding a thinner plasma. With this drop in ionization, the neutral density can begin to rise once again, allowing the process to restart. Fluid simulations that resolve low-frequency oscillations often find a "neutral tide" that ebbs and flows in time with discharge current fluctuations, consistent with this predator-prey picture.[8,10]

This process is captured with the zero-dimensional ion and neutral continuity equations,

$$\frac{dn}{dt} = \xi_{iz} n n_n - n\frac{u_i}{L} \tag{1}$$

and

$$\frac{dn_n}{dt} = -\xi_{iz} n n_n + n_n\frac{u_n}{L} \quad , \tag{2}$$

where n is the plasma density, n_n is the neutral gas density, u_i is the ion velocity, u_n is the neutral gas velocity, and ξ_{iz} is the ionization rate coefficient. A linear perturbation analysis of this system readily yields the following expression for breathing frequency ω:

$$\omega = \frac{\sqrt{u_i u_n}}{L} \quad . \tag{3}$$

As Barral and Ahedo noted,[13] this formulation is inaccurate because it does not account for neutral particles flowing into the region from the channel gas injector, $n_{n,0}$, regardless of injector geometry. Accounting for that and other slight discrepancies, Hara et al. produced the following expressions, where the first is equivalent to Fife's result in the limit of low growth:

$$\Re(\omega) = \sqrt{n n_n \xi^2 - \gamma^2} \quad , \tag{4}$$

$$\Im(\omega) \equiv \gamma = -\frac{1}{2}\frac{n_{n,0}}{n_{n,0} - n_n} n\xi \quad . \tag{5}$$

The major successes of these models is that they predict reasonable real frequencies, typically $\mathcal{O}$(1-10 kHz). However, there are severe limitations for both of these two variations of the predator-prey model. In Eq. (3), there is no imaginary component of ω, indicating the linear instability is metastable. In the presence of real-world damping processes, this implies these oscillations cannot be sustained in a real thruster. Similarly, Eq. (5) must be negative from physical constraints, and thus the linear oscillations are naturally damped.

Hara et al. investigated the role of electron energy in breathing oscillations with 0D and higher-order direct-kinetic modeling.[14,15] Although they found that a modified predator-prey model could linearly grow,[14] following studies showed on analytical grounds that the positive growth criteria are unphysical.[16] The closeness of the real frequencies predicted by the predator-prey model has generally led it to be a popular description of the breathing mode, yet its failure to predict growth – even with the addition of electron physics – suggests a few possibilities. First, the breathing mode may be a kinetic process that is poorly represented by fluid equations. Second, it may be a spatially-dependent phenomenon that is poorly represented with a 0D framework. Third, the surprising accuracy of Eq. (3) may indicate that the breathing process is primarily driven by neutral and ion behavior but there is an additional energy source sustaining the instability that is unrelated to the electron dynamics of the ionization region. In this study, we embrace this last option as being most plausible.

B. Higher-Order Ionization Instability

Barral, Ahedo, and Peradzynski adapted a 1D fluid model to a quasi-steady formulation that does not indiscriminately exclude temporal terms but instead encapsulates them with constant terms ${I_d}^{-1}dI_d/dt$ and n/I_d.[17,18] Numerical studies of this model matched the low-frequency oscillations of the fully time-dependent version but ignored higher frequency effects, like ion transit-time oscillations.[19] A linear analysis of the quasi-steady model suggested the presence of a standing plasma wave, $\tilde{n}/n \approx \tilde{I}_d/I_d$, as well as a lagging standing neutral wave combined with a traveling component,

$$\omega\tilde{n_n} \approx \tilde{I_d}\left(f_{iz}n_n - f_{iz,0}n_{n,0}\mathrm{Exp}\left[-i\frac{\omega z}{u_n}\right]\right) \quad , \tag{6}$$

for an effective ionization frequency $f_{iz,0}$. The second term in parentheses in Eq. (6) represents the standing component with wavenumber ω/u_n, while the parenthetical factor $\tilde{I_d}$ contributes a traveling component. It was intractible to estimate the growth rate analytically, but an order of magnitude analysis for the real frequency yielded

$$\Re(\omega) = \frac{u_i}{L}\mathcal{O}\left(\sqrt{\frac{n_n}{n}}\right) \quad , \tag{7}$$

which is equivalent to Eq. (3) within the bounds of Barral et al.'s model.

Because this model was developed as a simplification of a full set of 1D fluid equations, the physical interpretation was mostly added *a posteriori*. However, Barral and Ahedo interpreted their findings as depicting the typical neutral tide cycling forward and backward, accompanied by an oscillating ionization front. In short, they describe predator-prey action that includes spatial variation of the ionization zone and traveling fluctuation of the neutral population upstream of the ionization region.

The major success of this model is that, due to the relationship between the fully time-dependent model and quasi-steady model, it incontrovertibly predicts growing nonlinear low-frequency oscillations. Further, the similar scaling of ω with the traditional predator-prey model means that it too

will predict realistic frequencies. However, the lack of explicit physical insight provided by this approach limits its usefulness. Further, the complexity of the analysis owing to its 1D framework limits the practical benefits it offers. Combined, the lack of a defined physical mechanism to describe the instability – and in particular an explanation of where the 1D predator-prey process draws energy – puts the burden of proof on the theoretical results, but they too are obscure. As a result, it is difficult to accept Barral et al.'s model.

C. Near-Anode Effects

Numerical studies of the breathing mode have usually been either qualitative – typically noting that the observed features appear to be consistent with a predator-prey process – or have performed sensitivity studies on the instability. As an example of the latter, Hara et al. examined electron dynamics with a hybrid-direct kinetic code and found that the breathing mode is stabilized by reduced axial electron drift, possibly due to the formation of space charge saturated sheaths on the walls, and electron excitation becoming more significant than electron impact ionization.[11] However, they noted over all that suppression of electron energy and ionization near the anode tended to damp oscillations. This presaged fluid simulations by Hara and Mikellides where breathing behavior was found to depend on a wide variety of parameters, including electron mobility in the near-anode region.[20]

In general, there is mounting evidence that the anode plasma may contribute to development of the breathing mode. In the context of Hara et al.'s numerical studies, it was speculated that the effective ionization region may extend deep into the channel, and so reductions in ionization near the anode are shortening L in Eq. (3). Additionally, changes in near-anode electron mobility – independent of downstream mobility – may alter the potential structure in the channel, cooling the plasma and possibly initiating breathing oscillations due to the reduced wall heat flux.

The beauty of a breathing mode description involving upstream plasmadynamics is that it provides a simple growth mechanism for the predator-prey process. Instead of relying on nebulous spatial effects, the unique physics of the anode presheath, near-anode electron transport, and the anode sheath provide new opportunities for an energy source for the breathing mode. This explanation, though, is still firmly a result of numerical sensitivity and does not present a coherent physical process for the development of low-frequency oscillations.

III. Theory

A. Synthesis

To reiterate Section IIA, the simple predator-prey analysis suggests that the breathing mode may either be kinetic, spatially-dependent, or an ionization instability with an energy source outside the downstream ionization region. The fact that fluid simulations can reproduce these oscillations casts doubt on the first option. Interestingly, the last two options are not mutually exclusive. In Section IIB, we saw that a one-dimensional approach is more successful in capturing growing low-frequency oscillations than zero-dimensional. However, the scarcity of details in this higher-order ionization instability prevents us from determining whether the spatial dependence alone is sufficient to capture the breathing mode. But the studies described in Section IIC more definitively indicate that the spatial dependence may only be part of the growth mechanism. That is, the breathing mode was found to be sensitive to plasma properties in the near-anode region in ways that are not entirely consistent with the moving ionization front and standing plasma/neutral waves of Barral et al.'s 1D quasi-steady model. Altogether, this information can be used as the foundation for a simpler, more rigorous model for the breathing mode. The major lessons that will be taken into account are as follows:

1) The physical mechanism of the predator-prey model is qualitatively correct, and it is also fairly quantitatively accurate in describing the real frequency of oscillations.
2) A 1D model is capable of recovering low-frequency oscillations but is often analytically intractable, even with quasi-steady simplifications.
3) Regardless of the spatial dependence of the model, the near-anode region may need to be involved to correctly capture breathing oscillations.

B. Two-Zone Model

In the following we propose a two-zone predator-prey model that accounts for the lessons of the previous section. To motivate this derivation, we start by exploring the (corrected) predator-prey model of Fife et al. A linear perturbation analysis of Eqs. (1) and (2) produces a quadratic in ω, where $\alpha \equiv n_{n,0}/n_n$:

$$\omega^2 + \frac{i\alpha u_n \omega}{L} - (\alpha - 1)\frac{u u_n}{L^2} = 0 \quad . \tag{8}$$

Since there is only one imaginary term, the growth rate must either be zero or, by physical constraints, negative. This suggests that that other fluctuation terms out of phase with plasma and neutral density fluctuations, $\tilde{n}$ and $\tilde{n_n}$, must be included to allow for growth purely on analytical grounds. If we presume that the incoming neutral density $n_{n,0}$ is fluctuating such that $\tilde{n_{n,0}} = \mathcal{N}_n \tilde{n}$, where $\mathcal{N}$ is a complex amplitude, the linear perturbation quadratic becomes

$$\omega^2 + \frac{i\alpha u_n \omega}{L} - (\alpha - 1)u_n \frac{u_i - \mathcal{N}_n u_n}{L^2} = 0 \quad . \tag{9}$$

This quadratic has a closed form solution but isolating the imaginary frequency $\Im(\omega)$ is quite difficult, so the Routh-Hurwitz theorem can be employed to provide criteria for stability of the oscillations based on the number of stable and unstable roots:

$$\frac{i\alpha u_n}{L} > 0 \tag{10}$$

and

$$-(\alpha - 1)u_n \frac{u_i - \mathcal{N}_n u_n}{L^2} > 0 \quad . \tag{11}$$

The system is not stable if $u_i > u_n \Re(\mathcal{N}_n)$ and/or $\Im(\mathcal{N}_n) < 0$, where we assume $\alpha > 1$ and $u_n > 0$. Physically, these conditions suggest the oscillations *may* grow if $n_{n,0}$ fluctuates weakly in phase with n, out of phase with n, or leads n by any amount. In short, fluctuations of the incoming neutral density to the ionization/acceleration region may be sufficient for a predator-prey description of the breathing mode to predict growth.

This result is somewhat unprecedented in studies of 0D breathing models. It indicates that complicated physics do not need to be piled onto the traditional predator-prey model to yield growth. Rather, more fluctuating terms are only required to achieve this. However, this revelation is deceptively simple in that the process producing fluctuations in n_n needs to be modeled and incorporated into the 0D predator-prey framework. Based on the lessons of Section IIIA, we propose that the fluctuation in $n_{n,0}$ is a result of ionization in the near-anode region, coupling spatially to the predator-prey action at the downstream ionization zone.

1. Physical Process

We start first with a description of a hypothetical physical process based on the discussions of Section II, and then we explore it analytically in the following sections.

We presume that a predator-prey-like ionization instability exists in the traditional ionization zone. As the plasma density increases during rampant ionization, an excess of electrons stream to the anode. Ionization in the near-anode region is enhanced by this increase in electron flux. As a result, the neutral population is reduced, so a dearth of neutrals drift downstream. These neutrals reach the ionization region while the ionization rate there is already dropping due to typical predator-prey action, which exacerbates the drop. Once the plasma thins, a dearth of electrons stream to the anode, leading to an excess of neutrals drifting to the ionization region. In this way, the process repeats itself. A diagram of this process is provided in Fig. 1.

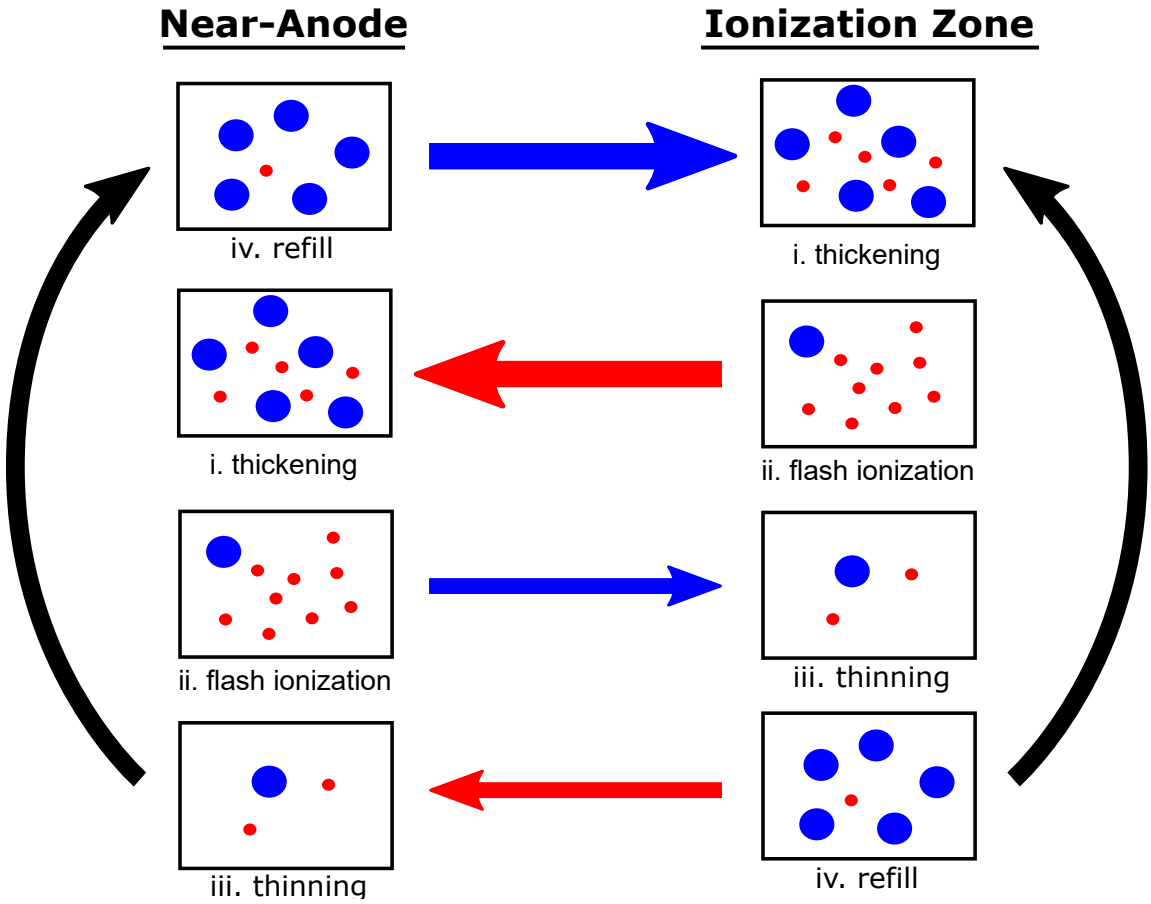

Fig. 1 A diagram of the physical process proposed for the two-zone model, where electrons are shown in red and neutral gas is shown in blue. The righthand cycle represents the typical predator-prey process in the ionization region, and the lefthand cycle represents a similar phenomenon near the anode. The arrows between the two reflect the coupling between the two instabilities.

Fundamentally, this model proposes that there are two coupled ionization instabilities, one in the traditional ionization region and one near the anode, and that it is the interplay between them that allows the otherwise predator-prey-like mechanism to grow. The energy for the instability is therefore derived from the electrons – it is the energy stripped from them during impact ionization events near the anode that supports fluctuations in the upstream neutral density, which in turn fuels the downstream predator-prey oscillations. An important aspect of this process is the delay in electrons reaching the anode from the ionization region, and the delay of neutrals reaching the ionization region from the anode. Presumably these quantities play a significant role in setting the

pace of breathing oscillations. The electron transit time is hard to predict in the near-anode region, and is often determined non-classically here. This adds an unfortunate complication to an otherwise very simple model. This implications of this will be discussed later in Section IV.

2. Model Derivation

We implement this hypothetical process as a two-zone predator-prey model. That is, we consider two coupled 0D sets of continuity equations, for ions and neutrals in the traditional ionization zone, and for electrons and neutrals near the anode. The evolution of the plasma and neutral populations is largely ignored between these zones, and instead we represent the transit of electrons and neutral particles between the zones with phasors $\mathcal{N}_{\rceil}\angle\theta_n$ and $\mathcal{N}_n\angle\theta_{n_n}$. The plasma density, neutral density electron velocity, and ionization rate coefficient near the anode are denoted n_a, $n_{n,a}$, $u_{e,a}$, and $\xi_{iz,a}$, respectively. The relevant 0D continuity equations assuming quasi-neutrality are as follows:

$$\frac{dn}{dt} = \xi_{iz} n n_n - n\frac{u_i}{L} \tag{12}$$

$$\frac{dn_n}{dt} = -\xi_{iz} n n_n + (n_{n,a} - n_n)\frac{u_n}{L} \tag{13}$$

$$\frac{dn_a}{dt} = \xi_{iz,a} n_a n_{n,a} + (n - n_a)\frac{u_{e,a}}{\lambda_D} \tag{14}$$

$$\frac{dn_{n,a}}{dt} = -\xi_{iz,a} n_a n_{n,a} + (n_{n,0} - n_{n,a})\frac{u_n}{\lambda_D} \tag{15}$$

Here, we assume that the neutral velocity does not vary spatially, that no ionization or acceleration occurs between the two regions, and that the near-anode region is contained with the anode sheath. The assumption of quasi-neutrality breaks down near the anode, but we ignore that here under the assumption that sheath potentials will be somewhat low so only a small disparity in densities exists. Also, it is important to note that the electron continuity equation pertains solely to electrons produced in the ionization region – electrons streaming from cathode to anode are ignored. In reality, recombination at the walls and other effects may limit the number of electrons that belong to this neglected group. In fact, we expect that the current utilization efficiency is a good representation of the ratio of channel-born to cathode-born electrons; these efficiencies are usually around 80% for modern thrusters,[21] which indicates that a minority of electron flux in the channel is sourced from the cathode.

Linearizing these equations yields the following system:

$$\begin{bmatrix} -i\omega & (1-\eta_1)\frac{u_n}{L} & 0 & 0 \\ \frac{u_{e,a}}{L} & -i\omega + \frac{u_n}{L} & 0 & -\mathcal{N}_{n_n}\angle\theta_{n_n}\frac{u_n}{L} \\ -\mathcal{N}_{\rceil_n}\angle\theta_n\frac{u_{e,a}}{\lambda_D} & 0 & -i\omega + (2-\eta_2)\frac{u_{e,a}}{\lambda_D} & (1-\eta_3)\frac{u_n}{\lambda_D} \\ 0 & 0 & (1-\eta_2)\frac{u_{e,a}}{\lambda_D} & -i\omega + \eta_3\frac{u_n}{\lambda_D} \end{bmatrix} \times \begin{bmatrix} \widetilde{n} \\ \widetilde{n_n} \\ \widetilde{n_a} \\ \widetilde{n_{n,a}} \end{bmatrix} = 0 \tag{16}$$

Here, the η quantities are density ratios: $\eta_1 \equiv n_{n,a}/n_n > 1$, $\eta_2 \equiv n/n_a < 1$, and $\eta_3 \equiv n_{n,0}/n_{n,a} > 1$. Physically, η_1 is the ratio of neutral density near the anode to that in the ionization region, which should be above unity due to ionization. Correspondingly, η_2 is the ratio of plasma density in the ionization region to that near the anode, where it should be below unity due to ionization. Finally, η_3 is the ratio of neutral density coming from anode to that near the anode, which we anticipate to be slightly above unity.

The solution of this system is a fourth-order polynomial in ω. Although closed-form solutions for polynomials like this exist, they are notoriously complicated and in this case would not avail an insightful solution. However, assuming $\eta_1 \gg 1$, $\eta_2 \ll 1$, and $\eta_3 \approx 1$, the following somewhat simplified equation results:

$$\begin{aligned} 0 = &\left\{ \frac{\eta_1 u_{e,a} {u_n}^2}{{\lambda_D}^2 L^2} [u_i(3\eta_3 - 1) + u_{e,a}\mathcal{N}_1 \angle\theta_n \mathcal{N}_n \angle\theta_{n_n}] \right\} \\ -i\omega &\left\{ \frac{\eta_1 u_n}{{\lambda_D}^2 L^2} [L u_{e,a} u_n (3\eta_3 - 1) + u_i \lambda_D (2u_{e,a} + u_n \eta_3)] \right\} \\ -\omega^2 &\left\{ \frac{u_n}{{\lambda_D}^2 L^2} [L^2 u_{e,a}(3\eta_3 - 1) + L\lambda_D \eta_1 (2u_{e,a} + u_n \eta_3) + \eta_1 {\lambda_D}^2 u_i] \right\} \\ +i\omega^3 &\left\{ \frac{1}{\lambda_D L} [L(2u_{e,a} + u_n \eta_3) + u_n \lambda_D \eta_1] \right\} \\ +\omega^4 & \end{aligned} \tag{17}$$

It is immediately apparent that several common terms appear in these coefficients. Further, there are some physical relationships between the quantities involved that may simplify the coefficients even further. In particular, we consider $u_{e,a} > u_i \gg u_n$, and we define $\delta \equiv \lambda_D / L$. Finally, since the phasor quantities appear together and if we assume that the transit of particles between zones is lossless, we combine them as $\angle\theta$. This reduces the equation to the following:

$$\begin{aligned} 0 = &\left\{ \frac{\eta_1 u_{e,a} {u_n}^2}{\delta^2 L^4} [u_i(3\eta_3 - 1) + u_{e,a}\angle\theta] \right\} \\ -i\omega &\left\{ \frac{\eta_1 u_{e,a} u_n}{\delta^2 L^3} [u_n(3\eta_3 - 1) + 2u_i\delta] \right\} \\ -\omega^2 &\left\{ \frac{u_n u_{e,a}}{\delta^2 L^2} [(3\eta_3 - 1) + 2\eta_1\delta] \right\} \\ +i\omega^3 &\left\{ \frac{1}{\delta L} [2u_{e,a} + u_n \eta_1 \delta] \right\} \\ +\omega^4 & \end{aligned} \tag{18}$$

3. Stability Analysis

The stability of this model can be evaluated aided by certain additional assumptions. First, we examine the low-growth limit $\Re(\omega) \gg \Im(\omega)$. Without making any assumptions on θ, the real component of Eq. (18) is a sparse quartic and the imaginary component a sparse cubic. Even though the latter is more tractable, complications still arise. For example, at a minimum the discriminant Δ of the polynomial can reveal the nature of any possible roots but here the sign of Δ is not immediately clear because the first-order coefficient has a different sign than the zeroth and third. However, an order of magnitude analysis suggests that $\Delta \ll 0$, which means that there is only one valid root to the cubic in this case. A large ω contradictorily yields $\omega = 0$, but a small ω compared to the zeroth order coefficient assuming $u_{e,a} \gg u_i$ and assuming $\eta_1\delta$ is relatively small yields

$$\Re(\omega) = \sqrt[3]{\frac{\eta_1 u_{e,a} {u_n}^2}{2\delta L^3}} \quad . \tag{19}$$

In summary, the only readily available solution for Eq. (18) in the limit of small growth requires $\sin(\theta)$ must be relatively large. This suggests that neutral particles must significantly lead/lag in phase while traveling from the anode to the ionization zone. However, note that we have assumed

$\Im(\omega)$ is small compared to $\Re(\omega)$, which itself is small compared to the zeroth order term of Eq. (18). We will return to this assumption in Section IV.

Next, the limit of high growth is investigated, $\Re(\omega) \ll \Im(\omega)$. In this case, the polynomial is a full and real quartic. To make any analytical progress, we assume θ is near $\pm 90°$; that is, the neutral particles accrue a considerable lead/lag in phase traveling through the channel. As a result, only the zeroth-order coefficient of Eq. (18) has an imaginary component. In fact, $\sin(\theta)$ must be zero in this case, which violates the starting premise that there is considerable lag/lead. Over all, then, the high growth limit is either unphysical or requires completely in-phase or out-of-phase θ, which is not consistent with the argument developed in Eq. (9). As a result, it seems likely that the growth rate predicted by this two-zone predator-prey model must be small or comparable to the real frequency.

IV. Results

As the previous section showed, only limited analytical information can be gleaned from Eq. (18) due to its complexity without severe assumptions. Alternatively, we can examine the linearized model numerically using realistic input parameters to evaluate its stability behavior.

A. Steady-State Quantities

The choice of steady-state quantities with which to explore the two-zone model must be given thought. For operation at 300 V and 15 A with 15 mg/s of xenon flow – a standard condition for the thruster tested in Part II of this study – the ion terminal velocity is roughly 20 km/s based on energy conservation and a typical voltage utilization efficiency of 93%.[21] For a symmetric E_z profile, u_i in the "center" of the acceleration region is closer to $1/\sqrt{2}$ times the terminal velocity, or 14 km/s. Previous studies in similar thrusters have shown neutral velocities to be close to 300 m/s throughout much of the channel.[22] The electron velocity in the ionization/acceleration is difficult to estimate, but following the approach of Hara et al. and assuming a current utilization efficiency η_I of about 80%, $u_e \approx (u_i/\eta_I)(1-\eta_I/\sqrt{2})$, roughly 7.8 km/s. A similar approach cannot be taken near the anode, and in general estimating $u_{e,a}$ is quite difficult. As a result, we consider it a free variable in this numerical study. With this information, the steady-state forms of Eqs. (12) to (15), combined with current continuity, yield downstream neutral and ion densities of 1.9×10^{18} m^{-3} and 2.8×10^{17} m^{-3}, and near-anode neutral and ion densities of 1.3×10^{19} m^{-3} and 3.1×10^{17} m^{-3}. This then means that η_1 is 7.0, η_2 is 0.9, and η_3 is 1.1, which agrees with our previous assessment about their comparison with unity.

B. Stability

Based on the previous discussion and the derivation of the previous section, the free variables in this numerical analysis are θ_n, θ_{n_n}, and $u_{e,a}$. For simplicity, we assume $\theta_n = 0$, as we expect electrons to travel rapidly from the ionization region to the anode. We can then examine how the real and imaginary components of ω, dictated by Eq. (18), evolve as a function of θ_{n_n} and $u_{e,a}$. Figure 2 shows this for the fastest-growing of the quartic's four roots. Both the real frequency and growth rate vary several orders of magnitude over the domain of θ_{n_n} and $u_{e,a}$, and the appearance of discontinuities suggest that the root locus structure may contain loops or intersections.

It is interesting to note that there is a region of considerable growth for $u_{e,a}$ near 2 km/s where the real frequencies are close to the anticipated order of magnitude, $\mathcal{O}(10$ kHz). However, the real frequency and growth rate appear to be independent of θ_{n_n} in this area. But if we examine it closer, as in Fig. 3a, very clear trends become apparent. For $u_{e,a}$=2 km/s, the real frequency is clearly directly proportional to $\sin(\theta_{n_n})$, and the growth rate weakly proportional to $\cos(\theta_{n_n})$. Physically,

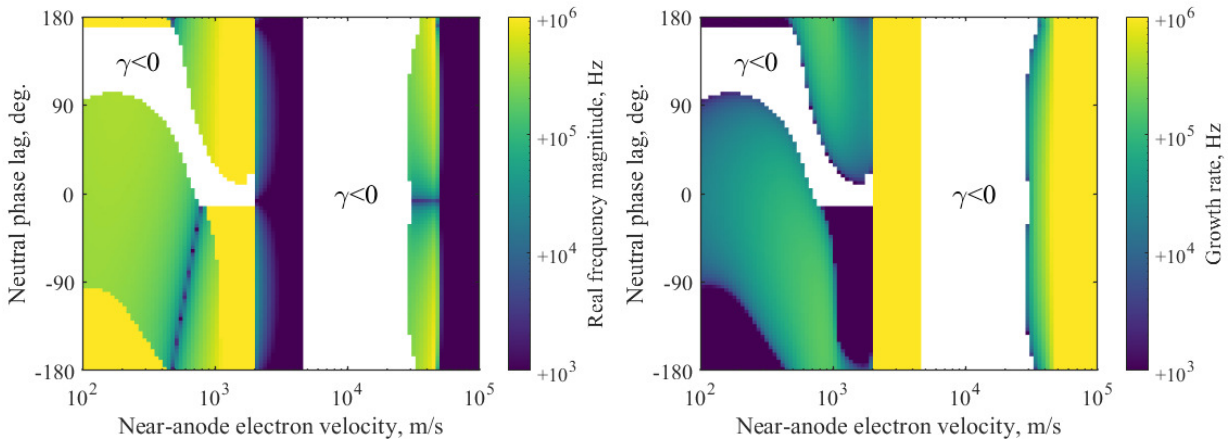

Fig. 2 The real frequency (a) and growth rate (b) as a function of neutral density phase lag and near-anode electron velocity. Damped regions are indicated on both plots with red dashed lines.

this indicates that the growth is strong regardless of θ_{n_n}, but the mode does not support linear oscillations when the neutral density fluctuations are completely in phase or out of phase during transit between zones.

Finally, Fig. 3b shows the root locus curves for $u_{e,a}$ of 2 km/s. These curves are traveled counterclockwise such that θ_{n_n} approaches 0° at their leftmost ends. As it shows, all four roots are always complex, with the limiting case that some of them become purely imaginary for θ_{n_n}=0. Further, it is interesting to note that there are in fact two growing roots. Although it is not apparent from Fig. 3b, the slower-growing root has higher real frequencies for a given θ_{n_n}, typically around twice as large as those of the fastest-growing root.

V. Discussion

Although the real frequency and growth rate vary intricately in Fig. 2, as we have pointed out in the previous section there appear to be regions of positive growth with real frequencies close to those anticipated for the breathing mode. In Section IIIB, we concluded that a lag/lead in the neutral particles as they transit the channel is sufficient for growth of a predator-prey instability, and in Section IIIB3 we found a similar result in the limit of low growth. However, the results of Fig. 3a make clear that for some $u_{e,a}$ the growth rate is much larger than the real frequency for all θ_{n_n}. In Section IIIB3, we had examined the high-growth limit and found it intractable, and in general such fast growth may suggest the process is highly non-linear. It is unclear, then, how well the results of the previous section describe the breathing mode.

To test this two-zone model more definitively, it is clearly important to verify that our guesses for steady-state parameters are correct. Further, it is critical to be able to estimate $u_{e,a}$ and θ_{n_n}, as the parameter space presented by these two quantities is too wide to be meaningful without experimental insight. For example, we focused on case of $u_{e,a}$ = 2 km/s, but according to Fig. 2 there are other values of $u_{e,a}$ that yield realistic ω, sometimes with more restrictive conditions on θ_{n_n}. Finally, it is important to verify that θ_n is small, as all of the numerical results examined here assume that.

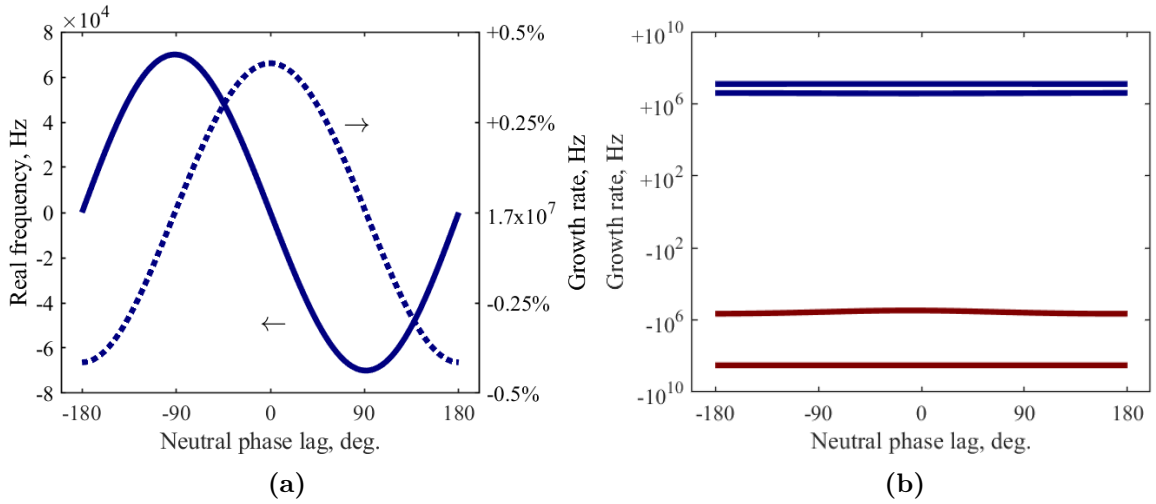

(a) **(b)**

Fig. 3 The real frequency and growth rate as a function of the neutral density phase lag (a), and the root loci of the two-zone model (b). Both plots assume $u_{e,a}$=0. In (a), the growth rate varies very little with θ_{n_n}, so the ordinate scale is in percentage change from the mean value. In (b), a signed logarithmic scale is used.

VI. Conclusions

In this work, an alternative model for the breathing mode involving two coupled ionization instabilities was developed. We found that allowing fluctuation of the neutral density entering the ionization zone may be sufficient for growth of the predator-prey model, which despite its shortcomings, is still prominent for its intuitiveness and passing quantitative accuracy. A physical mechanism was proposed wherein electron density excesses in the ionization region influence the ionization rate near the anode, which then alters the neutral density leaving the anode. This model was implemented analytically with ion and neutral continuity equations in the ionization zone, and electron and neutral continuity equations in the near-anode zone. Although the result was complicated, certain simplifying assumptions were made to explore its stability. Finally, a numerical study was performed that revealed many growing roots of the model, some of which correspond to real frequencies close to those expected for the breathing mode. In this way, a promising new model for the breathing mode has been presented, and numerical studies present encouraging correspondence with the breathing mode. This model will be investigated experimentally in Part II of this study.

References

[1] Oh, D. Y., Snyder, J. S., Goebel, D. M., Hofer, R. R., and Randolph, T. M., "Solar Electric Propulsion for Discovery-Class Missions," *Journal of Spacecraft and Rockets*, Vol. 51, No. 6, 2014, pp. 1822–1835.

[2] Dale, E. T. and Jorns, B. A., "Two-zone Hall thruster breathing mode mechanism, Part II: Experiment," *36th International Electric Propulsion Conference*, University of Vienna, Austria, Sept. 2019.

[3] Chesta, E., Lam, C. M., Meezan, N. B., Schmidt, D. P., and Cappelli, M. A., "A characterization of plasma fluctuations within a Hall discharge," *IEEE Transactions on Plasma Science*, Vol. 29, No. 4, Aug. 2001, pp. 582–591.

[4] Lobbia, R. B. and Gallimore, A. D., "High-speed dual Langmuir probe," *Review of Scientific Instruments*, Vol. 81, No. 7, July 2010, pp. 073503.

[5] Mazouffre, S. and Bourgeois, G., "Spatio-temporal characteristics of ion velocity in a Hall thruster discharge," *Plasma Sources Science and Technology*, Vol. 19, No. 6, 2010, pp. 065018.

[6] Young, C. V., Lucca Fabris, A., and Cappelli, M. A., "Ion dynamics in an EB Hall plasma accelerator," *Applied Physics Letters*, Vol. 106, No. 4, Jan. 2015.

[7] Sekerak, M. J., Gallimore, A. D., Brown, D. L., Hofer, R. R., and Polk, J. E., "Mode Transitions in Hall-Effect Thrusters Induced by Variable Magnetic Field Strength," *Journal of Propulsion and Power*, Vol. 32, No. 4, 2016, pp. 903–917.

[8] Boeuf, J. P. and Garrigues, L., "Low frequency oscillations in a stationary plasma thruster," *Journal of Applied Physics*, Vol. 84, No. 7, Oct. 1998, pp. 3541–3554.

[9] Adam, J. C., Héron, A., and Laval, G., "Study of stationary plasma thrusters using two-dimensional fully kinetic simulations," *Physics of Plasmas*, Vol. 11, No. 1, Jan. 2004, pp. 295–305.

[10] Parra, F. I., Ahedo, E., Fife, J. M., and Martínez-Sánchez, M., "A two-dimensional hybrid model of the Hall thruster discharge," *Journal of Applied Physics*, Vol. 100, No. 2, July 2006, pp. 023304.

[11] Hara, K., Sekerak, M. J., Boyd, I. D., and Gallimore, A. D., "Mode transition of a Hall thruster discharge plasma," *Journal of Applied Physics*, Vol. 115, No. 20, May 2014.

[12] Fife, J., Martinez-Sanchez, M., and Szabo, J., "A numerical study of low-frequency discharge oscillations in Hall thrusters," *33rd AIAA/ASME/SAE/ASEE Joint Propulsion Conference & Exhibit*, American Institute of Aeronautics and Astronautics, July 1997.

[13] Barral, S. and Ahedo, E., "On the Origin of Low Frequency Oscillations in Hall Thrusters," *AIP Conference Proceedings*, Vol. 993, AIP Publishing, March 2008, pp. 439–442.

[14] Hara, K., Sekerak, M. J., Boyd, I. D., and Gallimore, A. D., "Perturbation analysis of ionization oscillations in Hall effect thrusters," *Physics of Plasmas (1994-present)*, Vol. 21, No. 12, Dec. 2014.

[15] Hara, K., Boyd, I. D., and Kolobov, V. I., "One-dimensional hybrid-direct kinetic simulation of the discharge plasma in a Hall thruster," *Physics of Plasmas*, Vol. 19, No. 11, Nov. 2012, pp. 113508.

[16] Dale, E. T., Jorns, B., and Hara, K., "Numerical investigation of the stability criteria for the breathing mode in Hall Effect Thrusters," Atlanta, GA, Oct. 2017.

[17] Barral, S. and Ahedo, E., "Low-frequency model of breathing oscillations in Hall discharges," *Physical Review E*, Vol. 79, No. 4, April 2009.

[18] Barral, S. and Peradzyński, Z., "Ionization oscillations in Hall accelerators," *Physics of Plasmas (1994-present)*, Vol. 17, No. 1, Jan. 2010.

[19] Barral, S., Makowski, K., Peradzyński, Z., and Dudeck, M., "Transit-time instability in Hall thrusters," *Physics of Plasmas*, Vol. 12, No. 7, June 2005.

[20] Hara, K. and Mikellides, I. G., "Characterization of low frequency ionization oscillations in Hall thrusters using a one-dimensional fluid model," American Institute of Aeronautics and Astronautics, Cincinnati, Ohio, July 2018.

[21] Hofer, R., Goebel, D., Mikellides, I., and Katz, I., "Design of a Laboratory Hall Thruster with Magnetically Shielded Channel Walls, Phase II: Experiments," *48th AIAA/ASME/SAE/ASEE Joint Propulsion Conference & Exhibit*, American Institute of Aeronautics and Astronautics, Atlanta, GA, July 2012.

[22] Huang, W., Gallimore, A. D., and Hofer, R. R., "Neutral Flow Evolution in a Six-Kilowatt Hall Thruster," *Journal of Propulsion and Power*, Vol. 27, No. 3, May 2011, pp. 553–563.